PARAMETER ESTIMATION OF NON-RAYLEIGH RCS MODELS FOR SAR IMAGES BASED ON THE MELLIN TRANSFORMATION

Zengguo Sun, Chongzhao Han

School of Electronic and Information Engineering
Xi'an Jiaotong University
Xi'an, Shaanxi, P. R. China

ABSTRACT

The Mellin transformation-based method is developed to estimate the parameters of non-Rayleigh radar cross section (RCS) models for synthetic aperture radar (SAR) images from the observed image. Models investigated include heavy-tailed Rayleigh and Weibull. For each model, we consider the three kinds of images: intensity, square-root of intensity, and multi-look averaged amplitude. Using the Mellin transformation, we derive the analytical expressions of the first two second-kind cumulants for speckle and RCS respectively, and obtain the estimators according to the multiplicative model of SAR images and the Mellin convolution. Results of parameter estimation from Monte Carlo simulation and real SAR images demonstrate that the proposed estimators, which are easy to implement in the form of closed expressions, are efficient in estimating the parameters of non-Rayleigh RCS models from the observed SAR images.

***Index Terms*—** Synthetic aperture radar (SAR) images, non-Rayleigh RCS model, parameter estimation, Mellin transformation, Monte Carlo simulation

1. INTRODUCTION

The popular model for radar cross section (RCS) of SAR images is, of course, the Rayleigh model, which is based on the assumption that the radar resolution cell contains a large number of scatterers and none of the individual scatterers is significantly larger than the others [1]. However, the Rayleigh model is inapplicable for images such as a sparse forest or an urban scene observed by a high resolution radar [2]. In order to accurately model the RCS in such cases, several non-Rayleigh models have been proposed, including the heavy-tailed Rayleigh and Weibull. The heavy-tailed Rayleigh model is a generalization of the classical Rayleigh distribution [3]. With its heavier tails compared to the Rayleigh model, this model is a better choice for characterizing the high-resolution radar images of urban scenes and some natural scenes such as the sea surface [4]. The Weibull model contains the Rayleigh as a special case, and it is widely used for the modeling of ocean surface, land, weather, and sea-ice clutter [1, 2, 5].

One of the important problems in using these non-Rayleigh models in practical applications is how to estimate their parameters. This is not easy to achieve because the RCS is unknown to us and what we obtain is just the observed image. In [6], the Mellin transformation-based method is proposed to estimate the parameters of heavy-tailed Rayleigh RCS model from the observed intensity and square-root of intensity images. In this paper, we extend the Mellin transformation-based estimation to other non-Rayleigh model, and consider the commonly used multi-look averaged amplitude image for each model in addition to the intensity image and the square-root of intensity image [2, 7]. First, we derive the analytical expressions of the first two second-kind cumulants of speckle for the intensity image, the square-root of intensity image, and the multi-look averaged amplitude image. Since the speckle in the multi-look averaged amplitude image does not have the closed-form expression for the probability density function (pdf), we use the log-normal distribution to approximate the statistics of speckle, based on the premise that the log-transformed speckle is statistically very close to the Gaussian distribution [8]. We then derive the first two second-kind cumulants of the non-Rayleigh RCS models introduced above. Finally, based on the multiplicative model of SAR images and the Mellin convolution, we obtain the estimators which estimate the parameters of the non-Rayleigh RCS models directly from the observed image. The proposed estimators with the closed expressions are easy to implement with high estimation accuracy that is demonstrated by the parameter estimation experiments.

2. BRIEF INTRODUCTION OF MELLIN TRANSFORMATION AND SECOND-KIND CUMULANTS

The Mellin transformation of a function $f(x)$ ($x \geq 0$) is defined as [6]

$$\Phi(s) = \int_0^\infty x^{s-1} f(x)\, dx\,, \tag{1}$$

where s is the complex variable of the transformation. Based on the Mellin transformation, the r th order second-kind cumulant is defined by

$$\tilde{k}_r = \left. \frac{d^r \log \Phi(s)}{ds^r} \right|_{s=1}. \tag{2}$$

The commonly used multiplicative model of SAR images is given by [5-8]

$$y = x \cdot n\,, \tag{3}$$

where y is the observed image, x is the original image (RCS), and n is the speckle. According to the definition of the Mellin convolution, as stated in [6], the first two second-kind cumulants of y can be written as

$$\tilde{k}_{y(1)} = \tilde{k}_{x(1)} + \tilde{k}_{n(1)}, \qquad \tilde{k}_{y(2)} = \tilde{k}_{x(2)} + \tilde{k}_{n(2)}\,. \tag{4}$$

Here, $\tilde{k}_{x(r)}$ is the r th order second-kind cumulant of RCS, and $\tilde{k}_{n(r)}$ is the r th order second-kind cumulant of speckle. The first two second-kind cumulants of the observed image can be empirically estimated from the M observed samples y_i as follows:

$$\hat{\tilde{k}}_{y(1)} = \frac{1}{M}\sum_{i=1}^{M}\log y_i, \qquad \hat{\tilde{k}}_{y(2)} = \frac{1}{M-1}\sum_{i=1}^{M}\left(\log y_i - \hat{\tilde{k}}_{y(1)}\right)^2 . \quad (5)$$

Obviously, we can estimate the parameters of RCS models if we obtain the first two second-kind cumulants of speckle and RCS, which is shown in the following sections.

3. THE FIRST TWO SECOND-KIND CUMULANTS OF SPECKLE

In this section, the probability density function (pdf) of speckle is introduced for three kinds of SAR images: the intensity image, the square-root of intensity image, and the multi-look averaged amplitude image. We wish to obtain the first two second-kind cumulants of speckle for each case.

3.1. Intensity image

The pdf of speckle for the intensity image is given by the following Gamma distribution [6]

$$f(n) = \frac{L^L n^{L-1} e^{-Ln}}{\Gamma(L)} , \quad (6)$$

where L is the number of image looks, and $\Gamma(\cdot)$ is the Gamma function. Using (1) and (2), we can obtain the first two second-kind cumulants of speckle as follows:

$$\tilde{k}_{n(1)} = \psi(L) - \log L, \qquad \tilde{k}_{n(2)} = \psi(1, L) . \quad (7)$$

Here, $\psi(\cdot)$ is the Digamma function, and $\psi(1, L)$ is the first-order Polygamma function of L [8].

3.2. Square-root of intensity image

The pdf of speckle for the square-root of intensity image is given by the following Nakagami distribution [6, 8]

$$f(n) = \frac{2L^L n^{2L-1} e^{-Ln^2}}{\Gamma(L)} . \quad (8)$$

Similarly, we can obtain the first two second-kind cumulants of speckle by

$$\tilde{k}_{n(1)} = \frac{1}{2}(\psi(L) - \log L), \qquad \tilde{k}_{n(2)} = \frac{1}{4}\psi(1, L) . \quad (9)$$

3.3. Multi-look averaged amplitude image

The pdf of speckle for the multi-look averaged amplitude image is obtained by the multi-convolution of Rayleigh distribution, but, unfortunately, it cannot be expressed in a closed analytical form [7, 8]. However, it is demonstrated that the log-transformed speckle is statistically very close to the Gaussian distribution [8], so we can use the Gaussian model to approximate the log-transformed speckle N ($N = \log n$), which has the following pdf

$$f(N) = \frac{1}{\sqrt{2\pi}\sigma}\exp\left(-\frac{(N-\mu)^2}{2\sigma^2}\right), \quad (10)$$

where μ and σ^2 are the expectation and variance of this Gaussian distribution, respectively. Then, we can readily obtain the following pdf of n

$$f(n) = \frac{1}{\sqrt{2\pi}\sigma n}\exp\left(-\frac{(\log n-\mu)^2}{2\sigma^2}\right) . \quad (11)$$

In fact, the pdf above is just the log-normal distribution. We can easily obtain the expectation and variance of n from (11) as follows:

$$E(n) = \exp\left(\mu + \sigma^2/2\right), \qquad Var(n) = \exp\left(2\mu + 2\sigma^2\right) - \exp\left(2\mu + \sigma^2\right). \quad (12)$$

For the multi-look averaged amplitude image, we recall that [2]

$$E(n) = 1, \qquad Var(n) = 0.5227^2/L . \quad (13)$$

From (12) and (13), we can obtain

$$\mu = -\frac{1}{2}\log\left(1 + 0.5227^2/L\right), \qquad \sigma^2 = \log\left(1 + 0.5227^2/L\right). \quad (14)$$

From (11), using (1) and (2), we can derive the first two second-kind cumulants of speckle as follows:

$$\tilde{k}_{n(1)} = \mu, \qquad \tilde{k}_{n(2)} = \sigma^2 . \quad (15)$$

Substituting (14) into (15), finally, we have

$$\tilde{k}_{n(1)} = -\frac{1}{2}\log\left(1 + 0.5227^2/L\right), \qquad \tilde{k}_{n(2)} = \log\left(1 + 0.5227^2/L\right). \quad (16).$$

4. THE FIRST TWO SECOND-KIND CUMULANTS OF RCS

In this section, we model the RCS as the non-Rayleigh models such as the heavy-tailed Rayleigh and Weibull, and we derive the first two second-kind cumulants of each model for two kinds of SAR images: the amplitude image and the intensity image.

4.1. Heavy-tailed Rayleigh model

4.1.1. Amplitude image

The pdf of the heavy-tailed Rayleigh distribution for the amplitude image is given by

$$f(x) = x\int_0^\infty u\exp\left(-\gamma u^\alpha\right)J_0(ux)du , \quad (17)$$

where $0 < \alpha \le 2$ is the characteristic exponent, $\gamma > 0$ is the scale parameter, and $J_0(\cdot)$ is the zeroth order Bessel function of the first kind [4, 6]. Using (1) and (2), we can obtain the first two second-kind cumulants of RCS by

$$\tilde{k}_{x(1)} = \mathrm{C}_e\left(\frac{1}{\alpha} - 1\right) + \frac{\log\gamma}{\alpha} + \log 2, \qquad \tilde{k}_{x(2)} = \frac{\pi^2}{6\alpha^2} . \quad (18)$$

Here, C_e denotes the Euler's constant.

4.1.2. Intensity image

The pdf of the heavy-tailed Rayleigh distribution for the intensity image is given by [6]

$$f(x) = \frac{1}{2}\int_0^\infty u\exp\left(-\gamma u^\alpha\right)J_0\left(u\sqrt{x}\right)du . \quad (19)$$

Similarly, we can obtain the first two second-kind cumulants of RCS by

$$\tilde{k}_{x(1)} = 2\mathrm{C}_e\left(\frac{1}{\alpha} - 1\right) + \frac{2\log\gamma}{\alpha} + 2\log 2, \qquad \tilde{k}_{x(2)} = \frac{2\pi^2}{3\alpha^2} . \quad (20)$$

4.2. Weibull model

4.2.1. Amplitude image

The pdf of the Weibull distribution for the amplitude image is given by [5]

$$f(x)=\frac{cx^{c-1}}{b^c}\exp\left(-\left(\frac{x}{b}\right)^c\right), \tag{21}$$

where b is the scaling parameter, and c is the shape parameter. Using (1) and (2), we can obtain the first two second-kind cumulants of RCS by

$$\tilde{k}_{x(1)}=\log b-\frac{C_e}{c}, \qquad \tilde{k}_{x(2)}=\frac{\pi^2}{6c^2}. \tag{22}$$

4.2.2. Intensity image

From (21), we can obtain the pdf of the Weibull distribution for the intensity image by

$$f(x)=\frac{c\left(\sqrt{x}\right)^{c-2}}{2b^c}\exp\left(-\left(\frac{\sqrt{x}}{b}\right)^c\right). \tag{23}$$

Similarly, we can obtain the first two second-kind cumulants of RCS by

$$\tilde{k}_{x(1)}=2\log b-\frac{2C_e}{c}, \qquad \tilde{k}_{x(2)}=\frac{2\pi^2}{3c^2}. \tag{24}$$

5. MELLIN TRANSFORMATION-BASED ESTIMATORS

Since the first two second-kind cumulants are obtained for the speckle and the RCS, we can estimate the parameters of the RCS models directly from (4). We consider the heavy-tailed Rayleigh model as an example for the derivation. The parameter estimators for Weibull model can be derived similarly, so we omit the derivation steps and merely list the expressions for the estimators.

5.1. Heavy-tailed Rayleigh model

5.1.1. Intensity image

Substituting (5), (7), and (20) into (4), after some manipulation, we can obtain the following estimator for the intensity image

$$\begin{aligned}\hat{\alpha}&=\frac{\pi\sqrt{2}}{\sqrt{3\hat{\tilde{k}}_{y(2)}-3\psi(1,L)}}\\ \hat{\gamma}&=\exp\left\{\frac{\hat{\alpha}}{2}\left[\hat{\tilde{k}}_{y(1)}-2C_e\left(\frac{1}{\hat{\alpha}}-1\right)-2\log 2-\psi(L)+\log L\right]\right\}\end{aligned}. \tag{25}$$

5.1.2. Square-root of intensity image

Substituting (5), (9), and (18) into (4), after some manipulation, we can obtain the following estimator for the square-root of intensity image

$$\begin{aligned}\hat{\alpha}&=\frac{\pi}{\sqrt{6\hat{\tilde{k}}_{y(2)}-\frac{3}{2}\psi(1,L)}}\\ \hat{\gamma}&=\exp\left\{\hat{\alpha}\left[\hat{\tilde{k}}_{y(1)}-C_e\left(\frac{1}{\hat{\alpha}}-1\right)-\log 2-\frac{1}{2}\left(\psi(L)-\log L\right)\right]\right\}\end{aligned}. \tag{26}$$

5.1.3. Multi-look averaged amplitude image

As stated in [2], we still use the heavy-tailed Rayleigh distribution (17) to model the RCS for the multi-look averaged amplitude image. Substituting (5), (16), and (18) into (4), after some manipulation, we can obtain the following estimator

$$\begin{aligned}\hat{\alpha}&=\frac{\pi}{\sqrt{6\hat{\tilde{k}}_{y(2)}-6\log\left(1+\frac{0.5227^2}{L}\right)}}\\ \hat{\gamma}&=\exp\left\{\hat{\alpha}\left[\hat{\tilde{k}}_{y(1)}-C_e\left(\frac{1}{\hat{\alpha}}-1\right)-\log 2+\frac{1}{2}\log\left(1+\frac{0.5227^2}{L}\right)\right]\right\}\end{aligned}. \tag{27}$$

5.2. Weibull model

Using the Weibull distribution to model the RCS, the estimators are listed as follows for the three kinds of images.

For the intensity image,

$$\begin{aligned}\hat{c}&=\frac{\pi\sqrt{2}}{\sqrt{3\hat{\tilde{k}}_{y(2)}-3\psi(1,L)}}\\ \hat{b}&=\exp\left\{\frac{1}{2}\left[\hat{\tilde{k}}_{y(1)}+\frac{2C_e}{\hat{c}}-\psi(L)+\log L\right]\right\}\end{aligned}. \tag{28}$$

For the square-root of intensity image,

$$\begin{aligned}\hat{c}&=\frac{\pi}{\sqrt{6\hat{\tilde{k}}_{y(2)}-\frac{3}{2}\psi(1,L)}}\\ \hat{b}&=\exp\left[\hat{\tilde{k}}_{y(1)}+\frac{C_e}{\hat{c}}-\frac{1}{2}\left(\psi(L)-\log L\right)\right]\end{aligned}. \tag{29}$$

Finally, for the multi-look averaged amplitude image,

$$\begin{aligned}\hat{c}&=\frac{\pi}{\sqrt{6\hat{\tilde{k}}_{y(2)}-6\log\left(1+\frac{0.5227^2}{L}\right)}}\\ \hat{b}&=\exp\left[\hat{\tilde{k}}_{y(1)}+\frac{C_e}{\hat{c}}+\frac{1}{2}\log\left(1+\frac{0.5227^2}{L}\right)\right]\end{aligned}. \tag{30}$$

6. EXPERIMENTAL RESULTS

In this section, we provide the parameter estimation results from Monte Carlo simulation as well as real SAR images. We observe that the Mellin transformation-based estimators are efficient in estimating the parameters of the non-Rayleigh RCS models from the observed SAR images.

6.1. Monte Carlo simulation

Each Monte Carlo simulation is repeated 100 times independently, and the number of the samples is 10000 for each run. Using various image looks and true parameters, the parameter estimation results for these two RCS models (heavy-tailed Rayleigh and Weibull) are shown in Table 1 and Table 2, respectively. Obviously, for the three kinds of images, the proposed estimators can achieve high estimation accuracy no matter what values are chosen for the image looks and the true RCS parameters.

Table 1 Parameter estimation results of heavy-tailed Rayleigh model

Image Type	$L=1$				$L=4$			
	$\alpha=1 \quad \gamma=50$		$\alpha=1.5 \quad \gamma=500$		$\alpha=1 \quad \gamma=50$		$\alpha=1.5 \quad \gamma=500$	
	$\hat{\alpha}$	$\hat{\gamma}$	$\hat{\alpha}$	$\hat{\gamma}$	$\hat{\alpha}$	$\hat{\gamma}$	$\hat{\alpha}$	$\hat{\gamma}$
Intensity Image	0.9985	49.5595	1.5001	500.9917	1.0007	50.2355	1.4989	499.7688
Square-Root of Intensity Image	0.9995	49.9226	1.4984	499.4434	1.0012	50.2471	1.5001	501.3614
Multi-Look Averaged Amplitude Image	1.0003	50.1484	1.4990	499.4345	1.0021	50.3782	1.4993	499.8043

Table 2 Parameter estimation results of Weibull model

Image Type	$L=1$				$L=4$			
	$c=2 \quad b=100$		$c=4 \quad b=150$		$c=2 \quad b=100$		$c=4 \quad b=150$	
	$\hat{c}$	$\hat{b}$	$\hat{c}$	$\hat{b}$	$\hat{c}$	$\hat{b}$	$\hat{c}$	$\hat{b}$
Intensity Image	1.9927	99.9483	4.0219	150.1236	2.0005	100.0007	4.0045	149.9826
Square-Root of Intensity Image	1.9992	99.9602	4.0228	149.8499	1.9966	100.0699	3.9974	150.0149
Multi-Look Averaged Amplitude Image	2.0019	99.9007	4.0092	149.9188	1.9984	100.0384	3.9995	149.9612

6.2. Real SAR image experiments

The three kinds of SAR images are shown in Fig. 1, Fig. 2, and Fig. 3, respectively. For each image, we use the heavy-tailed Rayleigh and Weibull distributions to model the RCS. Then, we can estimate the parameters of the RCS models using the method proposed in this paper. The parameter estimation results for these three kinds of SAR images are shown in Table 3, Table 4, and Table 5, respectively. We can see that the proposed methods are efficient for the parameter estimation of the real SAR images.

Fig. 1 The intensity image for urban region ($L=10$)

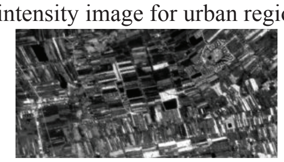

Fig. 2 The square-root of intensity image for rural region ($L=10$)

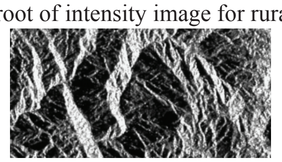

Fig. 3 The multi-look averaged amplitude image for mountain region ($L=4$)

Table 3 Parameter estimation results for the intensity image (Fig. 1)

Model	Estimated Parameters
Heavy-Tailed Rayleigh	$\hat{\alpha}=1.9412,\ \hat{\gamma}=25.2032$
Weibull	$\hat{c}=1.9412,\ \hat{b}=10.7289$

Table 4 Parameter estimation results for the square-root of intensity image (Fig. 2)

Model	Estimated Parameters
Heavy-Tailed Rayleigh	$\hat{\alpha}=1.8555,\ \hat{\gamma}=1114.5$
Weibull	$\hat{c}=1.8555,\ \hat{b}=91.7777$

Table 5 Parameter estimation results for the multi-look averaged amplitude Image (Fig. 3)

Model	Estimated Parameters
Heavy-Tailed Rayleigh	$\hat{\alpha}=1.1943,\ \hat{\gamma}=68.4640$
Weibull	$\hat{c}=1.1943,\ \hat{b}=101.6344$

7. CONCLUSIONS

In this paper, we estimate the parameters of commonly used non-Rayleigh RCS models from the observed SAR image based on the Mellin transformation. Our contribution can be summarized as follows: (1) we extend the Mellin transformation-based estimation to other non-Rayleigh model, and (2) we consider the commonly used multi-look averaged amplitude image for each model besides the intensity image and the square-root of intensity image. We focus our attention on the first two second-kind cumulants of speckle and the RCS, respectively. Particularly for the multi-look averaged amplitude image, we use the Gaussian distribution to approximate the statistics of the log-transformed speckle, then, we obtain the analytical closed-form expressions of the first two second-kind cumulants of speckle. Using the multiplicative model of SAR images and the Mellin convolution, we derive the parameter estimators with the closed forms for the non-Rayleigh RCS models. With the closed-form expressions and high estimation accuracy amply demonstrated by the parameter estimation experiments, the proposed estimators are efficient for estimating the parameter of the non-Rayleigh RCS models from SAR images.

8. REFERENCES

[1] M. I. Skolnik, *Introduction to Radar Systems, Third Edition*, McGraw-Hill, New York, 2001.

[2] F. T. Ulaby and M. C. Dobson, *Handbook of Radar Scattering Statistics for Terrain*, Artech House, Norwood, 1989.

[3] C. L. Nikias and M. Shao, *Signal Processing with Alpha-Stable Distributions and Applications*, Wiley, New York, 1995.

[4] E. E. Kuruoglu and J. Zerubia, “Modeling SAR images with a generalization of the Rayleigh distribution,” *IEEE Trans. Image Processing*, vol. 13, no. 4, pp. 527-533, Apr. 2004.

[5] C. Oliver and S. Quegan, *Understanding Synthetic Aperture Radar Images*, Artech House, Boston, 1998.

[6] A. Achim, E. E. Kuruoglu, and J. Zerubia, “SAR image filtering based on the heavy-tailed Rayleigh model,” *IEEE Trans. Image Processing*, vol. 15, no. 9, pp. 2686-2693, Sept. 2006.

[7] E. Hervet, R. Fjortoft, P. Marthon, and A. Lopes, “Comparison of wavelet-based and statistical speckle filters,” in *SPIE: SAR Image Analysis, Modeling and Techniques III*, vol. 3497, Barcelona, Spain, Sept. 1998.

[8] H. Xie, L. E. Pierce, and F. T. Ulaby, “Statistical properties of logarithmically transformed speckle,” *IEEE Trans. Geosci. Remote Sensing*, vol. 40, no. 3, pp. 721-727, Mar. 2002.